Obliquity pacing of the late Pleistocene glacial terminations

Peter Huybers[1] & Carl Wunsch[2]

[1] *Woods Hole Oceanographic Institution, Woods Hole, USA*

[2] *Massachusetts Institute of Technology, Cambridge, USA*

The timing of glacial/interglacial cycles at intervals of about 100,000 yr (100 kyr) is commonly attributed to control by Earth orbital configuration variations[1]. This "pacemaker" hypothesis has inspired many models[2–4], variously depending upon Earth obliquity, orbital eccentricity, and precessional fluctuations, with the latter usually emphasized. A contrasting hypothesis is that glacial cycles arise primarily because of random internal climate variability[5–7]. Progress requires distinguishing between the more than 30 proposed models of the late Pleistocene glacial variations[8]. Here we present a formal test of the pacemaker hypothesis, focusing on the rapid deglaciation events known as terminations[9,10]. The null hypothesis that glacial terminations are independent of obliquity can be rejected at the 5% significance level. In contrast, for eccentricity and precession, the corresponding null-hypotheses cannot be rejected. The simplest inference, consistent with the observations, is that ice-sheets terminate every second (80 kyr) or third (120 kyr) obliquity cycle—at times of high obliquity—and similar to the original Milankovitch assumption[11]. Hypotheses not accounting for the obliquity pacing are unlikely to be correct. Both stochastic and deterministic variants of a simple obliquity-paced model describe the observations.

To test whether the glacial variability is related to changes in Earth's astronomical configuration, we adopt a formal null-hypothesis (H_0) that glacial terminations are independent of obliquity variations, and the alternate hypothesis (H_1) that glacial terminations are paced by them. Our focus on obliquity is motivated by previous indications of nonlinear interactions between obliquity period and quasi-100 kyr glacial variability[12], but we also make identical tests for pacing by precession and eccentricity. We focus the test on glacial terminations because their magnitude and abruptness facilitate accurate identification.

Several obstacles must be overcome to distinguish between H_0 and H_1. A major problem is the need to establish time controls on the glacial variability. Many studies estimate age by assuming a relationship between climate proxy variability and orbital forcing[13,14], but this approach assumes the validity of the hypothesis being tested. Instead, we use an age-model devoid of orbital assumptions and apply it to the leading empirical orthogonal function (EOF1) of ten well-resolved marine $\delta^{18}O$ records[12], a proxy for ice-volume (Fig 1a).

Most simple models of the late Pleistocene glacial cycles have at least four degrees of freedom[2], and some have as many as twelve[3]. Unsurprisingly then, the seven observed quasi-100 kyr glacial cycles are insufficient to distinguish between the skill of the various models[15]. Models with minimal degrees of freedom are necessary. Other requirements for a useful test include the ability to cope with noisy records, age-model uncertainty, and (possibly) nonlinear interactions. Here we test for stability in the phase of the orbital parameters during glacial terminations using *Rayleigh*'s R (see Methods).

To proceed, we must estimate the probability distribution function associated with H_0. Of

the five estimation methods explored, we adopt the one which gives the highest critical value and thus makes H_0 the most difficult to reject — a modified random walk[7] representing ice-volume variability,

$$\begin{aligned} V_{t+1} &= V_t + \eta_t, \\ &\text{if } V_t \geq T_o, \text{ terminate.} \end{aligned} \tag{1}$$

This highly simplified model posits 1 kyr steps in ice-volume, V_t, of random length, η_t, independently drawn from a normal distribution with standard deviation $\sigma = 2$ and mean $\mu = 1$. The non-zero mean biasses the Earth toward glaciation. Once V_t reaches a threshold, $T_o = 90$, a termination is triggered, and ice-volume is linearly reset to zero over 10 kyr. If the model were deterministic with $\sigma = 0$ and $\mu = 1$, glacial cycles would last exactly 100 kyr, but with $\sigma = 2$, glacial cycle duration is approximately normally distributed at 100 ± 20 kyr, a spread consistent with observations[10]. Initial ice-volume is randomly set between 0 and T_o with equal probability. Using a Monte Carlo technique (see Methods) we find a critical value of $R = 0.60$ (Fig 1a,b).

The observed obliquity phases produce $R = 0.70$, and H_0 is rejected (Fig 1b). This rejection of H_0 is robust to all plausible reformulations of the test. Thus, the phase of obliquity has a statistically significant relationship with the timing of deglaciation. The mean phase direction is indistinguishable from zero and is associated with maxima in obliquity. We estimate the H_1 probability density function by assuming terminations always initiate at the same phase of obliquity, but that termination timing is subject to identification and age-model uncertainties (see Methods). The maximum likelihood value of H_1 is $R = 0.69$, very near the observed value, further supporting the conclusion that glacial terminations are paced by variations in obliquity.

Analogous hypothesis tests for precession and eccentricity produce different results. Age-model uncertainty approaches half a precession cycle, so that the power of the precession test is negligible — even if present, precession pacing of the glacial cycles cannot be discerned. In the case of eccentricity, H_0 is not rejected using the random walk probability estimate (Eq 1), but is rejected using weaker formulations of the eccentricity null-hypothesis. The discrepancy arises because null-hypotheses which assume a glacial timescale of roughly 100 kyr (which we consider to be more physical) tend to have higher R's and are more difficult to reject. As the hypotheses of negligible influence of precession and eccentricity on the glacial terminations cannot be rejected, we adopt a minimalist strategy, retaining only obliquity to describe the glacial terminations.

From a physical standpoint, support for the obliquity control hypothesis also comes from the fact that maxima in obliquity cause annual average insolation anomalies of up to 10 W/m^2 at high latitudes. Furthermore, the annual average and seasonal insolation redistributions associated with obliquity are hemispherically symmetric — as is the glacial variability to within a few thousand years[16,17]. Obliquity control of the glacial terminations also alleviates the marine isotope stage 11 problem[2] of explaining why termination 5 is large when the eccentricity and precession amplitude are small.

But how does a forcing with a 40 kyr period pace the 100 kyr late Pleistocene glacial variability? It appears the climate state skips one or two obliquity "beats" prior to deglaciating, giving quantized glacial cycle durations of either 80 or 120 kyr. One scenario is for increased obliquity to increase high-latitude insolation and cause heating of an ice-sheet, eventually warming the ice-bedrock interface. When the ice-sheet is small, basal temperature and pressure are

low, and the obliquity heating has little effect — a skipped beat. But when the ice-sheet is large, basal temperature and pressure are high[18], and the additional obliquity heating causes melting, lubricates the ice-flow, and triggers a termination. Note that $\sim$10 kyr is required for surface heating to penetrate to the base of an ice-sheet[18]. Unlike precession, changes in obliquity are associated with sustained annual average changes in insolation[19,20] and, thus, are more likely to cause basal warming of an ice-sheet. Furthermore, if climate was warmer during the early Pleistocene, terminations would be triggered more nearly every obliquity cycle, giving the observed smaller and more rapid glacial variability[21].

A simple system, consistent with the foregoing observations, is obtained by making the threshold in Eq 1 dependent on obliquity,

$$\begin{aligned} V_{t+1} &= V_t + \eta_t, \\ &\text{if } V_t \geq T_\circ - a\bar{\theta}_t, \text{ terminate.} \end{aligned} \tag{2}$$

Here $\bar{\theta}_t$ is obliquity[22], normalized to zero mean and unit variance, with amplitude a. The time variable threshold makes it more likely for a termination to occur when obliquity is large. We offer both deterministic and stochastic variants of Eq 2 to emphasize that such models are not theories of climate change, but rather attempts at efficient kinematic descriptions of the data, and that rather different mechanisms can be consistent with the limited observational records.

To make the model deterministic, the ice-volume step-size in Eq 2 is fixed at $\eta = 1$. Setting $a = 15$, $T_\circ = 105$, and (initial ice-volume) $V_{(t=-700)} = 30$ provides a good description of the late Pleistocene glacial variability (Fig 2a). Many other parameterizations yield similar results — we choose this one because it is particularly simple. The model produces the

correct timing of the glacial terminations (using termination 3a, not 3b) and has a squared-cross-correlation with $\delta^{18}O$ EOF1 of 0.65, an excellent fit considering there are only three adjustable parameters. (Adjustments made using η can equivalently be made using the other parameters.) For comparison, tuning other models having four[2] or twelve[3] adjustable parameters yields maximum squared-cross-correlations with EOF1 of 0.24 and 0.74 respectively[23]. If skill is measured by squared-cross-correlation divided by the number of adjustable parameters, Eq 2 does more than three times as well.

A periodogram of the deterministic model results (Fig 2b) shows narrow-band concentrations of energy at the average 100 kyr period, the 41 kyr obliquity period, and at previously identified[12] combination tones, 1/41-1/100=1/70, 1/41+1/100=1/29, and 1/41+2/100=1/23 kyr — in good agreement with the $\delta^{18}O$ EOF1 periodogram. The appearance of 1/23 kyr narrow-band energy in the absence of precession band forcing highlights the ambiguous origins of this energy band[20]. Note the model also has energy at 2/100 kyr, not visible in the observations. Also, while deterministic, the model produces an energetic background continuum consistent with the $\delta^{18}O$ periodogram.

For the stochastic case, η_t is defined to be normally distributed with $\sigma = 2$ and mean $\mu = 1$. Here η_t represents the unpredictable background weather and climate variability spanning all time scales out to the glacial/interglacial. All other parameter settings are kept the same as in the deterministic case. Now, Eq 2 resembles an order one autoregressive process. Such a process is known to well-describe the glacial variability, excepting "runs" associated with glacial terminations[24], here modeled using the threshold condition in Eq 2. The time between terminations in the stochastic model averages 100 kyr but has a tri-modal distribution with max-

ima at two (80 kyr), three (120 kyr), and four (160 kyr) obliquity cycles (Fig 2d). The observed durations between terminations are consistent with the dominant 80 and 120 kyr modes, but suggest that one would see 160 kyr glacial cycles, given a larger sample size. The R obtained by the stochastic model averages 0.85 (Fig 2e), higher than the observed $R = 0.70$, and as expected because of observational age-model error.

Deterministic and stochastic variants of Eq 2 thus both describe the late Pleistocene glacial variability. A description of the early Pleistocene variability[21] is obtained by lowering the termination threshold to $T_\circ = 40$, giving smaller amplitude terminations that occur more nearly every obliquity cycle. Alternatively, instead of specifying a parameter change, the mid-Pleistocene transition can be described using a chaotic model[23] (not shown) having spontaneous transitions between 40 and 100 kyr modes of glacial variability. At this point, it is unclear whether adequate data will ever be available to distinguish between stochastic, simple deterministic, and chaotic deterministic models of the glacial variability.

The simplest interpretation of our results is that, during the Pleistocene, Earth tends to a glacial state (anthropogenic influences aside) but deglaciates at obliquity maxima. Obliquity control of the timing of deglaciation, probably in concert with a stochastic forcing, has several other consequences. These include inferences drawn from precession and eccentricity based models of glaciation[25], the hemispheric symmetry of glacial cycles, and the efficacy of age-model tuning of cores. These issues will be taken up elsewhere.

Methods

Rayleigh's R is defined as[26]

$$R = \frac{1}{N}\left|\sum_{n=1}^{N} \cos\phi_n + i\sin\phi_n\right|. \quad (3)$$

Here, ϕ_n is the phase of obliquity stroboscopically sampled at the nth glacial termination. The $|.|$ indicate the magnitude, making R real and non-negative, with a maximum value of one when the phases are all equal. Relative to other measures of phase coupling used to investigate cardiac synchronization[27] and a wide range of other nonlinear interactions[28], Rayleigh's R requires many fewer phases (roughly five) to test for phase stability[26].

To measure R between obliquity and the glacial cycles, we use $\delta^{18}O$ EOF1 and an age-model independent of orbital assumptions[12] (Fig 1a). Such an independent age-model is important because even so-called minimal tuning strategies — using only a narrow-band of a climate record — tend to align the abrupt glacial terminations with a particular phase of the assumed forcing (as indicated by Monte Carlo simulations), thus biasing records towards H_1.

The rate of change of EOF1 has a unimodal distribution with a long tail, indicative of rapid melting. Terminations are defined to initiate when the rate of change in EOF1 first exceeds the two-standard deviation level. This criterion identifies each of the usual terminations[9,10], but two events in the termination 3 deglacial sequence, termed 3a and 3b for the younger and older events respectively. Additional rules could be added to exclude 3a or 3b, but this rejection seems ad hoc, and we use all eight termination events. Note, the timing of termination 3 predicted by the Paillard model[3] also coincides with either event 3a or 3b, depending on slight changes in the parameterizations. Reassuringly, results are not sensitive to details of the test: either termination

3a or 3b can be excluded; termination times can be defined using the midpoint between the local minimum and maximum bracketing each termination; and individual benthic or planktic $\delta^{18}O$ records[14] can be used in place of EOF1.

The probability density function (PDF) associated with H_0 is estimated using the modified random walk model (Eq 1). A realization of R is obtained by sampling the phase of obliquity at eight consecutive termination initiations, generated from Eq 1, and the PDF of H_0 is estimated by binning 10^4 such realization of R. Other methods are to assume a uniform phase distribution, use surrogate data techniques[29], or to derive statistics from ensemble runs of other models, but all these give PDF estimates which make H_0 more easily rejected and are therefore not used.

To estimate the PDF associated with H_1, we assume that glacial terminations always occur at the same phase of obliquity, but that the phase observations are subject to identification and age-model error. A Monte Carlo technique is used where the timing of the glacial terminations are perturbed according to the estimated age uncertainties[12] (these average ± 9 kyr) and identification error (± 1 kyr, the EOF1 sampling resolution). A realization of R is then computed using the phase of obliquity at the perturbed ages, and 10^4 such realizations are binned to estimate the PDF of H_1. We estimate the likelihood of correctly rejecting $H_\circ$ (i.e. the power of the obliquity test) to be 0.57. See the supplementary web information for a listing of the pertinent data and statistics.

Bibliography

1. Hays, J., Imbrie, J. & Shackleton, N. Variations in the earth's orbit: Pacemaker of the ice ages. *Science* **194**, 1121–1132 (1976).

2. Imbrie, J. & Imbrie, J. Modeling the climatic response to orbital variations. *Science* **207**, 943–953 (1980).

3. Paillard, D. The timing of Pleistocene glaciations from a simple multiple-state climate model. *Nature* **391**, 378–391 (1998).

4. Gildor, H. & Tziperman, E. Sea ice as the glacial cycles' climare switch: Role of seasonal and orbital forcing. *Paleoceanography* **15**, 605–615 (2000).

5. Saltzman, B. Stochastically-driven climatic fluctuations in the sea-ice, ocean temperature, co2, feedback system. *Tellus* **34**, 97–112 (1982).

6. Pelletier, J. Coherence resonance and ice ages. *Journal of Geophysical Research* **108** (2003).

7. Wunsch, C. The spectral description of climate change including the 100ky energy. *Climate Dynamics* **20**, 353–363 (2003).

8. Saltzman, B. *Dynamical Paleoclimatology: Generalized Theory of Global Climate Change* (Academic Press, San Diego, 2002).

9. Broecker, W. Terminations. In Berger, A. & et. al. (eds.) *Milankovitch and climate, Part2*, 687–698 (D. Riedel, Hingham, 1984).

10. Raymo, M. E. The timing of major climate terminations. *Paleoceanography* **12**, 577–585 (1997).

11. Milankovitch, M. *Kanon der Erdbestrahlung und seine Andwendung auf das Eiszeiten-problem* (Royal Serbian Academy, Belgrade, 1941).

12. Huybers, P. & Wunsch, C. A depth-derived Pleistocene age-model: Uncertainty estimates, sedimentation variability, and nonlinear climate change. *Paleoceanography* **19** (2004).

13. Imbrie, J. & et. al. The orbital theory of Pleistocene climate: Support from a revised chronology of the marine delta 18 O record. In Berger, A. & et. al. (eds.) *Milankovitch and Climate, Part 1*, 269–305 (D. Riedel, Hingham, 1984).

14. Shackleton, N. J., Berger, A. & Peltier, W. R. An alternative astronomical calibration of the lower Pleistocene timescale based on ODP site 677. *Trans. R. Soc. Edinb.-Earth Sci.* **81**, 251–261 (1990).

15. Roe, G. & Allen, M. A comparison of competing explanations for the 100,000-yr ice age cycle. *Geophysical Research Letters* **26**, 2259–2262 (1999).

16. Blunier, T. & Brook, E. Timing of millennial-scale climate change in Antarctica and Greenland during the last glacial period. *Science* **291**, 109–112 (2001).

17. Wunsch, C. Greenland-Antarctic phase relations and millennial time-scale climate fluctuations in the Greenland cores. *Quaternary Science Reviews* **22**, 1631–1646 (2003).

18. Marshall, S. & Clark, P. Basal temperature evolution of North American ice sheets and impications for the 100-kyr cycle. *Geophysical Resarch Letters* **29** (2002).

19. Rubincam, D. Insolation in terms of earth's orbital parameters. *Theoretical Applied Climatology* **48**, 195–202 (1994).

20. Huybers, P. & Wunsch, C. Rectification and precession-period signals in the climate system. *Geophysical Research Letters* **30** (2003).

21. Raymo, M. & Nisancioglu, K. The 41 kyr world: Milankovitch's other unsolved mystery. *Paleoceanography* **18(1)** (2003).

22. Berger, A. & Loutre, M. F. Astronomical solutions for paleoclimate studies over the last 3 million years. *Earth Planet. Sci. Lett.* **111**, 369–382 (1992).

23. Huybers, P. *On the Origins of the Ice Ages: Insolation Forcing, Age Models, and Nonlinear Climate Change*. Ph.D. thesis, MIT (2004).

24. Wunsch, C. Quantitative etimate of the Milankovitch-forced contribution to observed quaternary climate change. *Quaternary Science Reviews* **23**, 1001–1012 (2004).

25. Ruddiman, W. F. Orbital insolation, ice volume, and greenhouse gases. *Quaternary Science Reviews* **22**, 1597–1622 (2003).

26. Upton, G. & Fingleton, B. *Spatial Data Analysis by Example*, vol. 2 (John Wiley and Sons, Chichester, 1989).

27. Schafer, C., Rosenblum, M., Kurths, J. & Abel, H. Heartbeat synchronized with ventilation. *Nature* **34**, 239–240 (1998).

28. Rosenblum, M. & Pikovsky, A. Synchronization: from pendulum clocks to chaotic lasers and chemical oscillators. *Contemporary Physics* **44**, 401–416 (2003).

29. Schreiber, T. & Schmitz, A. Surrogate time series. *Physica D* **142**, 346–382 (2000).

Acknowledgments. Useful comments were provided by E. Boyle, W. Curry, Tim Herbert, J. McManus, M. Tingley, G. Yang, and two anonymous reviewers. PH is supported by the NOAA Postdoctoral Program in Climate and Global Change and CW in part by the National Ocean Partnership Program (ECCO).

Correspondence and requests for materials should be addressed to phuybers@whoi.edu.

Figure 1 The Rayleigh test for phase directionality. ***a***, $\delta^{18}O$ EOF1 normalized so that negative values indicate more ice. Dots indicate onset of a termination and horizontal bars indicate one-standard-deviation age-model uncertainties[12]. Termination 3 is split between events 3a and 3b. Vertical lines indicate the time of maxima in obliquity. ***b***, The obliquity phase (dots) sampled at each termination and plotted on a unit circle. The vector average has a magnitude, $R = 0.70$ (cross mark), exceeding the critical value, $c = 0.60$ (filled circle), so that H_0 is rejected. Furthermore, R is near H_1's maximum likelihood value (dashed circle). The direction is indistinguishable from maximum obliquity (top of the circle). Analogous tests are made for ***c*** precession ($R = 0.43$, $c = 0.60$) and ***d*** eccentricity ($R = 0.66$, $c = 0.84$), but in neither case can the corresponding H_0 be rejected. See the supplementary web information for more details.

Figure 2 Deterministic and stochastic descriptions of the late Pleistocene glacial variability. ***a*** Deterministic model results (red) with an obliquity dependent threshold (black) plotted over EOF1 (brown). ***b*** Periodograms of the deterministic model results (red) and EOF1 (brown). Concentrations of energy are centered on the 1/41 kyr obliquity frequency and the 1/100 kyr glacial band; as well as combination tones at 1/70, 1/29, and 1/23 kyr. The approximate 95% confidence interval is indicated by the vertical bar at right. ***c*** A realization of the stochastic model. ***d*** Histogram of time between terminations, derived from many runs of the stochastic model. The observed duration between terminations (triangles, using termination 3a not 3b) coincide with the dominant 80 and 120 kyr modes. ***e*** Histogram of Rayleigh's R from the stochastic model with the observed obliquity value, R=0.70, indicated by the triangle.

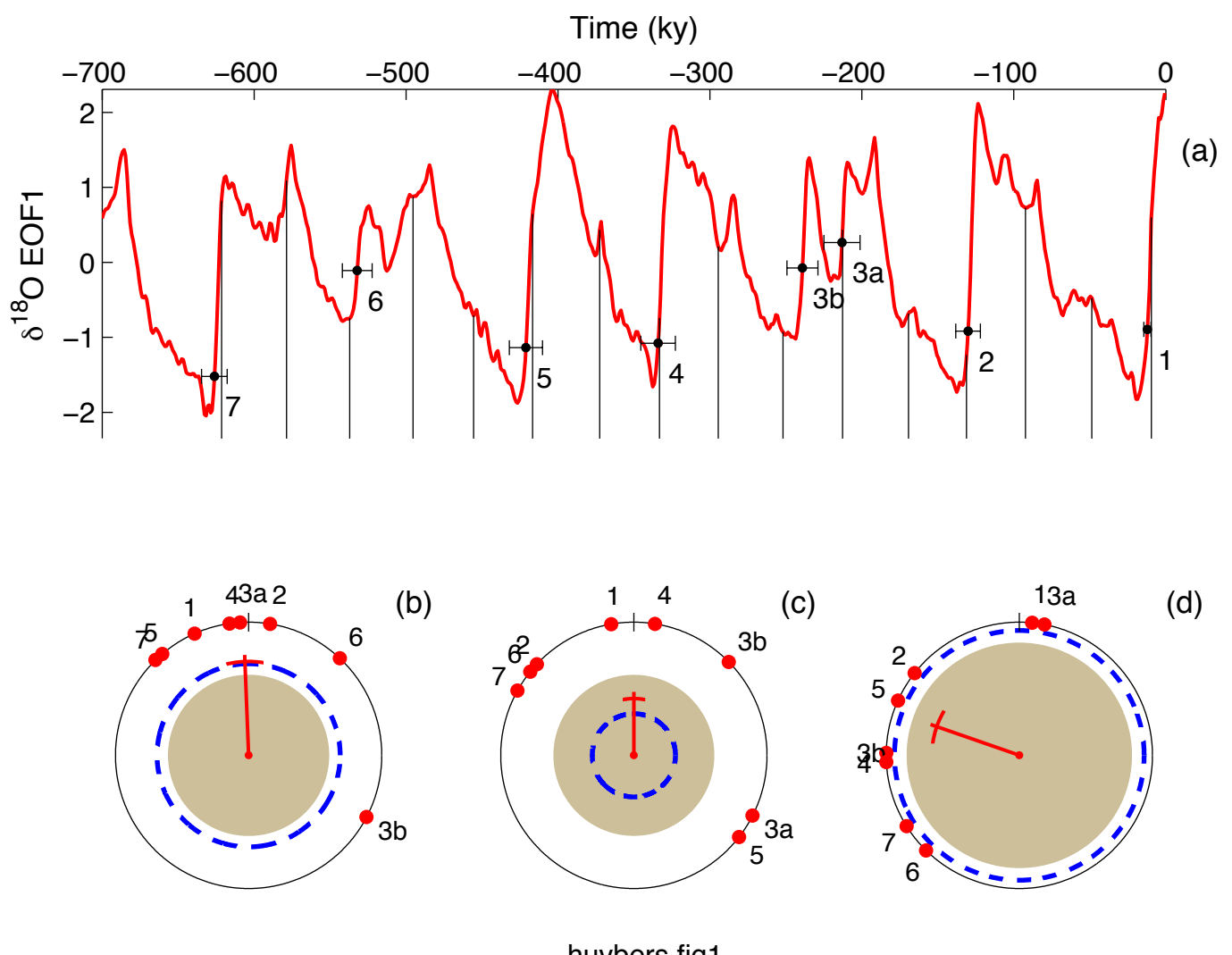
Time (ky)
−700
−600
−500
−400
−300
−200
−100
0
2
1
0
−1
−2
δ18O EOF1
(a)
7
6
5
4
3b
3a
2
1
(b)
1
4
3a
2
5
7
6
3b
(c)
1
4
2
6
7
3b
3a
5
(d)
13a
2
5
3b
4
7
6
huybers fig1

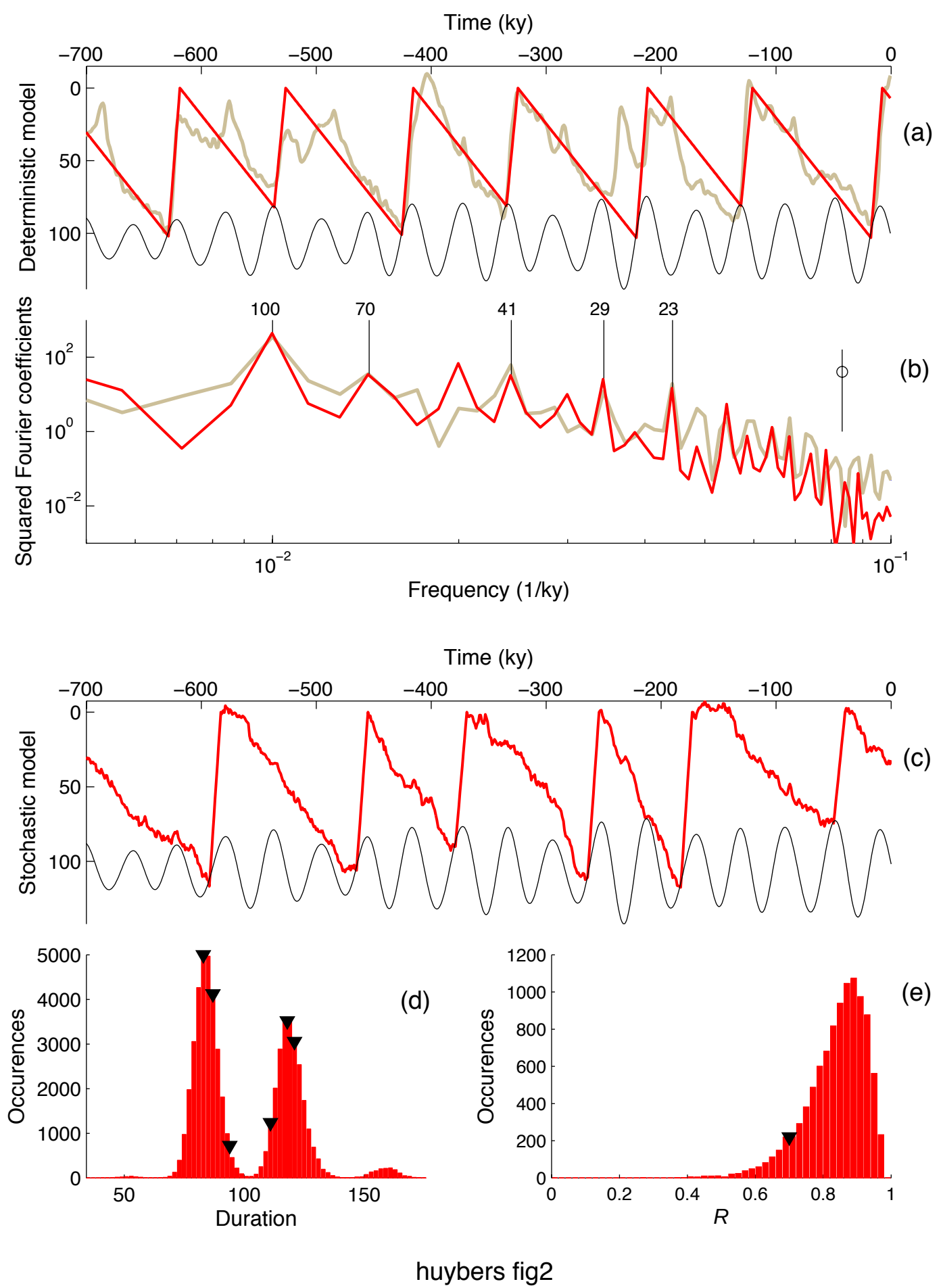

huybers fig2